k · p calculations of p-type δ-doped quantum wells in Si

Isaac Rodríguez-Vargas [a,*], Miguel E. Mora-Ramos [b]

[a] *Unidad Académica de Física, Universidad Autónoma de Zacatecas, Calzada Solidaridad Esquina Con Paseo La Bufa S/N, 98060 Zacatecas, ZAC., Mexico*
[b] *Facultad de Ciencias, Universidad Autónoma del Estado de Morelos, Av. Universidad 1001, Col. Chamilpa, 62210 Cuernavaca, MOR., Mexico*

Abstract

We present the hole subband structure calculation in single and double p-type δ-doped quantum wells in Si based on the 4×4 Luttinger–Kohn Hamiltonian. The valence band bending and the Γ hole states are calculated within the lines of the Thomas–Fermi–Dirac approximation and the effective mass theory at the Brillouin zone center. The obtained zone center eigenstates are then used to diagonalize the **k · p** Hamiltonian for non-zero **k**. The hole subband structure is analyzed as a function of the impurity density and the distance between δ wells. It is shown that the application of a 4×4 model to describe the hole ground state in single p-type δ-doped in Si can be misleading.

© 2008 Elsevier Ltd. All rights reserved.

Keywords: Hole subband structure; δ-doped quantum wells; **k · p** approximation

1. Introduction

Silicon is the leading semiconducting material regarding its technological applications. Additionally, some interesting properties are present in the so-called δ-doped systems. Studies of p-type B-δ-doped Si quantum wells have been reported [1–4]. B-δ-doped Si QW has been investigated from the theoretical and experimental points of view [1–12]. It is clear that in the case of p-type systems the simultaneous consideration of the heavy and light hole bands is unavoidable because the electric charge is distributed among them. Due to the technological importance of this material and the particular properties of the δ-doped systems, they appear to be of interest for application in the electronic device industry and for basic investigation as well (see for instance, [13,14], and references therein).

From the technological point of view double δ-doped (DDD) QWs offer an improvement in the transport properties with respect to single δ-doped (SDD) ones [15–20]. This improvement is of importance for possible implementation in high speed, amplifier, and switching devices, in which a high density charge -and consequently, mobility- is sought.

Due to those properties, a more complete and rigorous calculation of the hole subband structure of multiple p-δ-doped systems is necessary to understand the underlying physics behind these layered systems. The band bending profile is described analytically along the lines of the local density Thomas–Fermi–Dirac (TFD) approximation, including the exchange contribution [21,22]. With the derived model potential we have calculated the eigenstates and eigenfunctions at the Brillouin zone center. Then, this set of eigenstates are taken as a basis for the diagonalization of the 4×4 **k · p** Hamiltonian, thus obtaining the hole subband structure for $k \neq 0$, which is analyzed as a function of the doping density and the interwell distance.

2. Method and model

For a single δ-doped quantum well, a direct relation between the hole density $p(z)$ and the Hartree potential $V_H(z)$ was previously obtained in the one-dimensional

---

* Corresponding author. Tel./fax: +52 492 924 1314.
E-mail address: issac@planck.reduaz.mx (I. Rodríguez-Vargas).

TFD approach within the local density approximation (LDA) [23]. It is written as

$$p_{au}(z) = \frac{m_a^3 \varsigma^3(w)}{3\pi^5} \left[1 - \sqrt{1 + \frac{\pi^2(\mu^* - V_H^*(z))}{\varsigma^2(w)m_a}} \right]^3, \qquad (1)$$

where $p_{au}(z)$, $V_H^* = V_H/R_y^*$ and $\mu^* = \mu/R_y^*$ are the hole density, the Hartree potential and the chemical potential in atomic units, respectively. $m_a = \left[1 + \left(\frac{m_{lh}}{m_{hh}} \right)^{3/2} \right]^{2/3}$, where m_{hh} and m_{lh} are the heavy and light hole masses, respectively. Effective heavy-hole-related Si atomic units are used throughout.

$\varsigma(w)$ accounts for the valence band coupling and is given by [24]

$$\varsigma(w) = 2^{-1/3} + (1 - w^2)[w^2(aw + b) + c(4w^3 + 3w^2 + 2w + 1)], \qquad (2)$$

where $w = \sqrt{m_{lh}/m_{hh}}$, $a = 0.679$, $b = -0.0686$ and $c = -0.0811$. By including Eq. (1) in the corresponding Poisson equation, an explicit expression for the Hartree potential centered in $z = d$ is obtained. It has the form

$$V_H^*(z) - \mu^* = -\frac{\alpha^2}{(\alpha|z - d| + z_0)^4}, \qquad (3)$$

with $\alpha = \frac{2m_a^{3/2}}{15\pi}$ and $z_0 = \left(\frac{\alpha^3}{\pi p_{2D}^{au}} \right)^{1/5}$. p_{2D}^{au} is the acceptor density in atomic units.

In the framework of the LDA, the exchange potential for a hole gas can be written as

$$V_x^*(z) = -\varsigma(w)\frac{2}{\pi}(3\pi^2)^{1/3}(p_{au}(z))^{1/3} \qquad (4)$$

Using the relation between $p_{au}(z)$ and $V_H(z)$ it is possible to write the total potential $V^* = V_H^* + V_x^*$ as

$$V^*(z) = -\frac{\alpha^2}{(\alpha|z - d| + z_0)^4} - \frac{2\varsigma^2(w)m_a}{\pi^2}\left[1 - \sqrt{1 + \frac{\pi^2}{\varsigma^2(w)m_a}\frac{\alpha^2}{(\alpha|z - d| + z_0)^4}} \right] \qquad (5)$$

The latter equation summarizes the model for the band bending profile. Instead of carrying out numerically troublesome self-consistent calculations, we simply solve three Schrödinger-like effective mass equations at the zone center **k = 0**, thus obtaining the corresponding ladders of the hole levels.

The construction of a model potential for the DDD is performed via an appropriate combination of two single δ-wells centered at $z = -l/2$ and $z = l/2$, considering the same impurity density in both doping spikes, as it has been reported in [21,22]. Again, the solutions of effective-mass Schrödinger equations, lead to the Brillouin zone center states for heavy and light holes.

The next step is the diagonalization of the 4×4 **k · p** Luttinger–Kohn Hamiltonian [25]. That is, we need to solve the secular problem

$$\begin{pmatrix} H^{hh} & b & c & 0 \\ b^* & H^{lh} & 0 & c \\ c^* & 0 & H^{lh} & -b \\ 0 & c^* & -b^* & H^{hh} \end{pmatrix} \begin{pmatrix} \phi_m^{3/2,3/2}(\vec{\kappa},z) \\ \phi_m^{3/2,1/2}(\vec{\kappa},z) \\ \phi_m^{3/2,-1/2}(\vec{\kappa},z) \\ \phi_m^{3/2,-3/2}(\vec{\kappa},z) \end{pmatrix}$$

$$= E^h(\vec{\kappa}) \begin{pmatrix} \phi_m^{3/2,3/2}(\vec{\kappa},z) \\ \phi_m^{3/2,1/2}(\vec{\kappa},z) \\ \phi_m^{3/2,-1/2}(\vec{\kappa},z) \\ \phi_m^{3/2,-3/2}(\vec{\kappa},z) \end{pmatrix} \qquad (6)$$

where $\phi_m^v(\vec{\kappa},z)$ is the function associated to the confining potential of the quantum wells. The components with $v = 3/2, \pm 3/2$ and $v = 3/2, \pm 1/2$ correspond to the heavy and light holes, respectively. m is the subband index and $E^h(\vec{\kappa})$ are the energy eigenvalues of the holes; i.e., the subbands. In effective atomic units, the matrix elements in Eq. (6) are given by

$$H^{hh} = -\left[\eta_1 \kappa^2 + \frac{\partial^2}{\partial z^2} \right] + V(z),$$

$$H^{lh} = -\left[\eta_2 \kappa^2 + \xi_1 \frac{\partial^2}{\partial z^2} \right] + V(z), \qquad (7)$$

$$b = -6i\xi_3(\sin\theta + \cos\theta)\kappa\frac{\partial}{\partial z},$$

$$c = 6i(\xi_2 \cos 2\theta - i\xi_3 \sin 2\theta)\kappa^2$$

with

$$\eta_1 = \frac{\gamma_1 + \gamma_2}{\gamma_1 - 2\gamma_2}, \quad \eta_2 = \frac{\gamma_1 - \gamma_2}{\gamma_1 - 2\gamma_2},$$

$$\xi_1 = \frac{\gamma_1 + 2\gamma_2}{\gamma_1 - 2\gamma_2}, \quad \xi_2 = \frac{\gamma_2}{\gamma_1 - 2\gamma_2}, \quad \xi_3 = \frac{\gamma_3}{\gamma_1 - 2\gamma_2}.$$

Here, γ_1, γ_2 and γ_3 are the Luttinger parameters, $\vec{\kappa} = (k_x, k_y)$ is the parallel wavevector in the $x - y$ plane of the well, θ is the angle between $\vec{\kappa}$ and the k_x-direction. $V(z)$ represents the confinement potential, which in our case is given by Eq. (5).

The technique chosen for this process consists in the use of the set of Γ-point wave functions as a basis for the expansion of the non-Γ-point states [26,27]. Mathematically this reads as follows: at the Γ point, $E^h(\vec{\kappa}) = E_{0m}^h$: the ladder of levels of the QW. At the same time, there is not any interband coupling ($b = c \equiv 0$) Eq. (7) is simplified to

$$H^{hh} = -\frac{\partial^2}{\partial z^2} + V(z)$$

$$H^{lh} = -\xi_1 \frac{\partial^2}{\partial z^2} + V(z), \qquad (8)$$

We can also write $\xi_1 = m_{hh}/m_{lh}$ provided that the effective masses of the heavy and light holes are defined as $m_{hh} = m_0/(\gamma_1 - 2\gamma_2)$ and $m_{lh} = m_0/(\gamma_1 + 2\gamma_2)$, respectively. In consequence Eq. (6) is reduced to two independent effective mass Schrödinger equations with eigenvalues E_0^{hh}, and E_0^{lh}, and eigenfunctions $\phi_{0m}^{3/2,\pm3/2}(z)$, and $\phi_{0m}^{3/2,\pm1/2}(z)$, for heavy and light holes, respectively.

At the Γ point the heavy-hole states $\phi_{0m}^{3/2,3/2}$, $\phi_{0m}^{3/2,-3/2}$ are degenerated and have the same quantized energies E_{0m}^{hh}. The same happens between $\phi_{0m}^{3/2,1/2}$, $\phi_{0m}^{3/2,-1/2}$ with quantized energies E_{0m}^{lh}. If the spin is not considered, $\phi_{0m}^{3/2,3/2}$ and $\phi_{0m}^{3/2,-3/2}$ are in fact the same solution, and so do $\phi_{0m}^{3/2,1/2}$ and $\phi_{0m}^{3/2,-1/2}$.

Now for k_x, $k_y \neq 0$, and b and $c \neq 0$ the mixing effects exist between the heavy and light hole bands. In order to solve the Luttinger–Kohn equation, Eq. (6) and obtain the hole eigenvalues and eigenfunctions at non-Γ points we take a basis for the energy representation that consists of the above eigenstates $\phi_{0m}^{v}(z)$ at Γ point. Then, it is proposed that the eigenfunctions sought, $\phi_{m}^{v}(\vec{\kappa}, z)$, can be expanded as

$$\phi_m^{3/2,3/2} = \sum_{l=1}^{n1} A_l \phi_{0l}^{3/2,3/2}, \quad \phi_m^{3/2,1/2} = \sum_{l=1}^{n2} B_l \phi_{0l}^{3/2,1/2}$$

$$\phi_m^{3/2,-1/2} = \sum_{l=1}^{n2} C_l \phi_{0l}^{3/2,-1/2}, \quad \phi_m^{3/2,-3/2} = \sum_{l=1}^{n1} D_l \phi_{0l}^{3/2,-3/2}$$

$$(9)$$

where n_1, n_2 are the numbers of energy eigenfunctions $\phi_{0l}^{3/2,\pm3/2}$, $\phi_{0l}^{3/2,\pm1/2}$ at the Γ point, respectively. A_l, B_l, C_l, D_l are the expanding coefficients. Multiplying Eq. (6) by the matrix

$$\left[\phi_m^{*3/2,3/2}, \phi_m^{*3/2,1/2}, \phi_m^{*3/2,-1/2}, \phi_m^{*3/2,-3/2} \right], \quad (10)$$

and substituting Eq. (9) into the result, and then integrating over z, it is possible to obtain the following energy matrix equation [26]:

$$\begin{pmatrix} \mathbf{H^{hh}} & \mathbf{b} & \mathbf{c} & \mathbf{0'} \\ \mathbf{b^\dagger} & \mathbf{H^{lh}} & \mathbf{0''} & \mathbf{c} \\ \mathbf{c^\dagger} & \mathbf{0''} & \mathbf{H^{lh}} & -\mathbf{b} \\ \mathbf{0'} & \mathbf{c^\dagger} & -\mathbf{b^\dagger} & \mathbf{H^{hh}} \end{pmatrix} \begin{pmatrix} \mathbf{A} \\ \mathbf{B} \\ \mathbf{C} \\ \mathbf{D} \end{pmatrix} = E^h \begin{pmatrix} \mathbf{A} \\ \mathbf{B} \\ \mathbf{C} \\ \mathbf{D} \end{pmatrix} \quad (11)$$

where $\mathbf{0'}$ and $\mathbf{0''}$ are the zero square matrices of n_1 and n_2 orders, respectively. The energy eigenvector $\mathbf{A}$, $\mathbf{B}$, $\mathbf{C}$ and $\mathbf{D}$ are given by

$$\mathbf{A} = \begin{pmatrix} A_1 \\ A_2 \\ \vdots \\ A_{n_1} \end{pmatrix} \quad \mathbf{B} = \begin{pmatrix} B_1 \\ B_2 \\ \vdots \\ B_{n_2} \end{pmatrix} \quad \mathbf{C} = \begin{pmatrix} C_1 \\ C_2 \\ \vdots \\ C_{n_2} \end{pmatrix} \quad \mathbf{D} = \begin{pmatrix} D_1 \\ D_2 \\ \vdots \\ D_{n_1} \end{pmatrix}$$

$$(12)$$

and the matrix elements of Eq. (11) come as

$$H_{l'l}^{hh} = \int_{-\infty}^{\infty} \phi_{0l'}^{*3/2,3/2} H^{hh} \phi_{0l}^{3/2,3/2} \, dz \quad (l', l = 1, 2, \ldots, n_1)$$

$$H_{l'l}^{lh} = \int_{-\infty}^{\infty} \phi_{0l'}^{*3/2,1/2} H^{lh} \phi_{0l}^{3/2,1/2} \, dz \quad (l', l = 1, 2, \ldots, n_2)$$

$$b_{l'l} = \int_{-\infty}^{\infty} \phi_{0l'}^{*3/2,3/2} b \phi_{0l}^{3/2,1/2} \, dz$$

$$(l' = 1, 2, \ldots, n_1, l = 1, 2, \ldots, n_2)$$

$$c_{l'l} = \int_{-\infty}^{\infty} \phi_{0l'}^{*3/2,3/2} c \phi_{0l}^{3/2,1/2} \, dz$$

$$(l' = 1, 2, \ldots, n_1, l = 1, 2, \ldots, n_2) \quad (13)$$

The computation of the coefficient matrix in Eq. (11) is needed to obtain the quantized energy values E_m^{hh} and $E_{m'}^{lh}$ as well as their corresponding relative energy eigenvectors $\mathbf{A}$, $\mathbf{B}$, $\mathbf{C}$ and $\mathbf{D}$ for heavy and light holes at the non-Γ states.

3. Results and discussion

In the present work we limit ourselves to study the hole subband structure of the two-dimensional hole gas in Si SDD and DDD QW for doping densities of the order of 5×10^{12} cm^{-2} (here we switch back to normal units) and below. This justifies the fact of considering only the contributions from the heavy and light hole bands, and corresponds to the range of most reported densities in GaAs-based δ-doped systems. For these values of p_{2D} the inclusion of the split-off band in the Hartree potential $V_H(z)$ through a contribution of the form $\left(\frac{m_{so}}{m_{hh}} \right)^{3/2}$ in the averaged effective mass parameter m_a, does not result in practically any difference in the spectrum of levels, compared to the present case.

There is an uncertainty in the literature with respect to the values of the Luttinger parameters for Si. We choose to consider two different sets herein: I; $\gamma_1 = 4.285$, $\gamma_2 = 0.339$, $\gamma_3 = 1.446$, is taken from the experimental determination quoted by Hensel as a private communication in Ref. [28] (see also Ref. [6]). II; $\gamma_1 = 4.25$, $\gamma_2 = 0.37$, $\gamma_3 = 1.46$, is obtained from a report on Dresselhaus–Kane parameters given in Ref. [29]. In addition, the static dielectric constant is taken to be $\epsilon_r = 11.7$. All energies presented throughout this section are measured with respect to the Γ-point valence band edge.

Figs. 1 and 2 show the potential well profiles and -schematic- $\mathbf{k} = 0$ single-hole confined states of Si p-type δ-doped quantum wells in for a doping concentration of 5×10^{12} cm^{-2}. The Fig. 1 corresponds to the set of Luttinger parameters (SLP) labeled as I, while 2 depicts the case of SLP II. In fact, very small quantitative differences regarding the potential well's depths as well as the values of the energy levels are found when using one SLP or the other. We obtain for the mentioned concentration (all in meV) the following values related to single δ-doped quantum wells: $V_0 = 67.3$, $E_{hh0} = 26.7$, $E_{hh1} = 1.8$, $E_{lh0} = 24$, for the SLP I, and $V_0 = 66.5$, $E_{hh0} = 26.1$, $E_{hh1} = 1.6$, $E_{lh0} = 23.7$ for the SLP II.

As it should be expected, for the same concentration the levels of double δ-doped quantum wells are deeper and in both SLPs the state lh1 becomes well localized.

In Fig. 3 we can see the energy dispersion relations for the hole subbands in single Si p-type δ-doped quantum
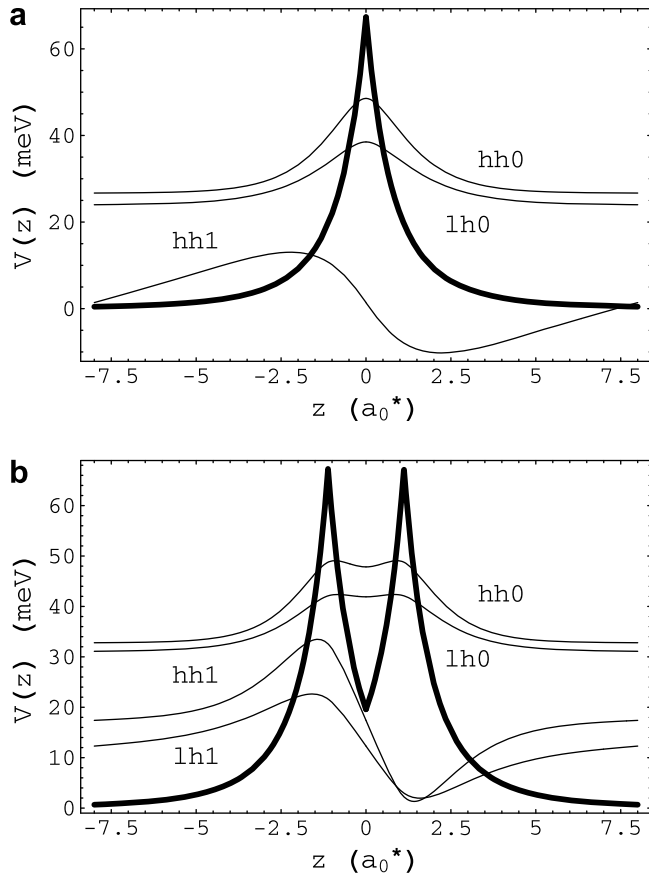
Fig. 1. Potential well profiles and (schematic) single-hole states, corresponding to the motion along the direction of quantum well confinement, for p-type δ-doped quantum wells in Si for a doping concentration of 5×10^{12} cm^{-2}. (a) Single δ-doped quantum well. (b) Double δ-doped quantum well with interwell distance equals to 50 Å. This figure corresponds to the set of Luttinger parameters labeled as **I**.

Fig. 2. The same as in Fig. 1 but for the set of Luttinger parameters labeled as **II**.

wells. The figure is obtained for a two-dimensional doping concentration $p_{2D} = 5 \times 10^{12}$ cm^{-2}. The corresponding subband dispersion relations (a) and (b) are calculated with the use of the SLPs **I** and **II**, respectively. No important differences between cases (a) and (b) can be noticed for both directions considered in the two-dimensional Brillouin zone. Furthermore no appreciable orientation-related anisotropy is detected in both cases.

Fig. 4 shows the energy dispersion curves for a p-type Si double δ-doped quantum well with $l = 50$ Å are presented for SLP **I** (a) and SLP **II** (b), for a doping concentration $p_{2D} = 2.5 \times 10^{12}$ cm^{-2}. The change in the SLP used does not reflect onto significant differences. But the effect of intersubband mixing comes out in this case, particularly in the [110]-direction. This results in a warping of the higher subbands that leads to a negative effective mass behavior. In the case of the ground state (hh0), this behavior starts very close to the zone center. The reason for this to happen relies in the aforementioned fact that the hole states become more localized and therefore their interaction strengthens. The difference between directions [100] and [110] comes specially from the "c" element in the Lutt-
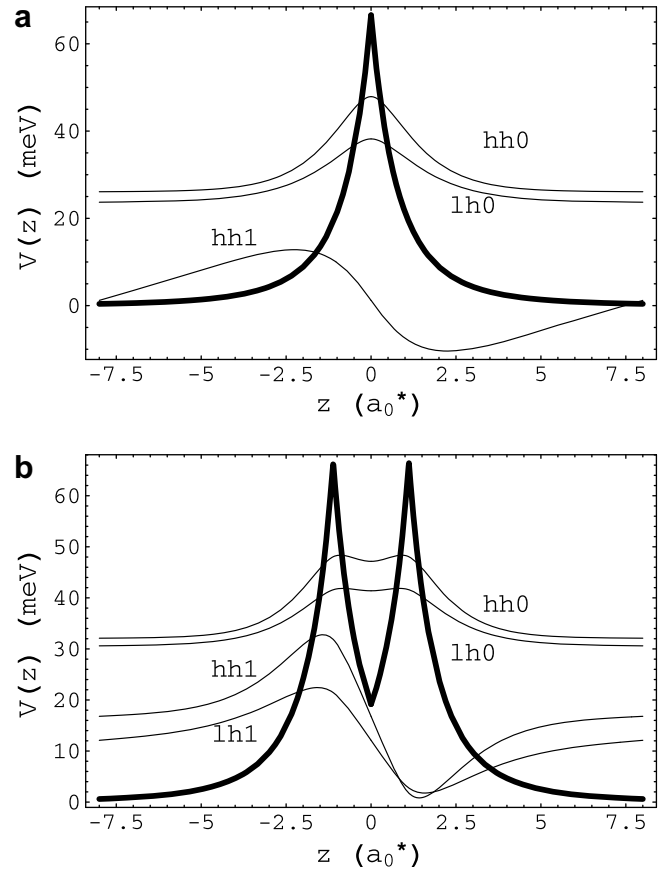
inger–Kohn Hamiltonian which substantially changes for it goes from depending on γ_2 to depends on γ_3, together with a change in sign. This is seen in the set of graphs included in Fig. 5, which shows the evolution in the subband structure as depending on the values of θ, going from small to close to $\pi/4$. For any other direction, from 0 to $\pi/4$ (or equivalent, due to the fourfold symmetry), both γ_2 and γ_3 contribute to"c". The parameter γ_2 is predominant in Eq. (7) for directions corresponding to small angles (for instance, the direction [1 2 1 0], shown in Fig. 5a, that corresponds to approximately 5°). In the case of directions associated to intermediate values of the angle θ, both parameters contribute almost with the same weight. Finally, in the case of directions with angles close to $\pi/4$, γ_3 is predominant (an example is the [1 2 1 1 0] direction shown in Fig. 5h, which corresponds to an angle of 42°).

It can be also seen that the energetic distance between lh0 and hh1 is smaller in the double well compared with its value in the single δ-doped one; hence the strong anti-crossing seen in the figures for $\kappa \approx 0.5$ nm^{-1}. The κ and energy positions of this anti-crossing slightly shifts toward smaller values of the 2D wavevector and higher values of the energy, respectively, as long as the direction in the Brillouin zone approaches $\theta = \pi/4$.

Fig. 6 shows the dispersion relations for p-type Si double δ-doped quantum wells with $p_{2D} = 5 \times 10^{12}$ cm^{-2}, for
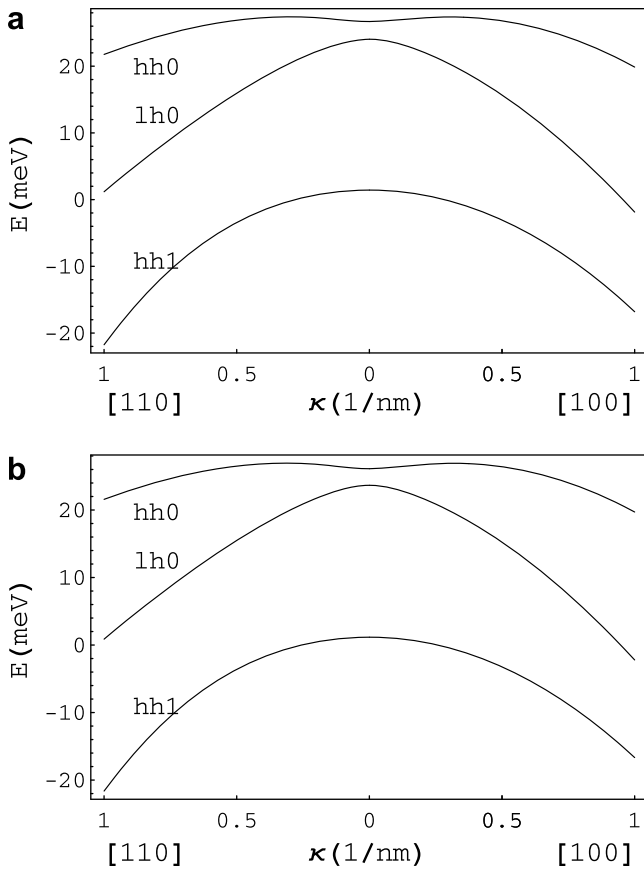
Fig. 3. Energy dispersion along two directions in the two-dimensional Brillouin zone for single p-type δ-doped Si quantum wells with doping density $p_{2D} = 5 \times 10^{12}$ cm^{-2}. (a) Corresponds to the set of Luttinger parameters labeled as **I**, while (b) corresponds to the set named as **II**.
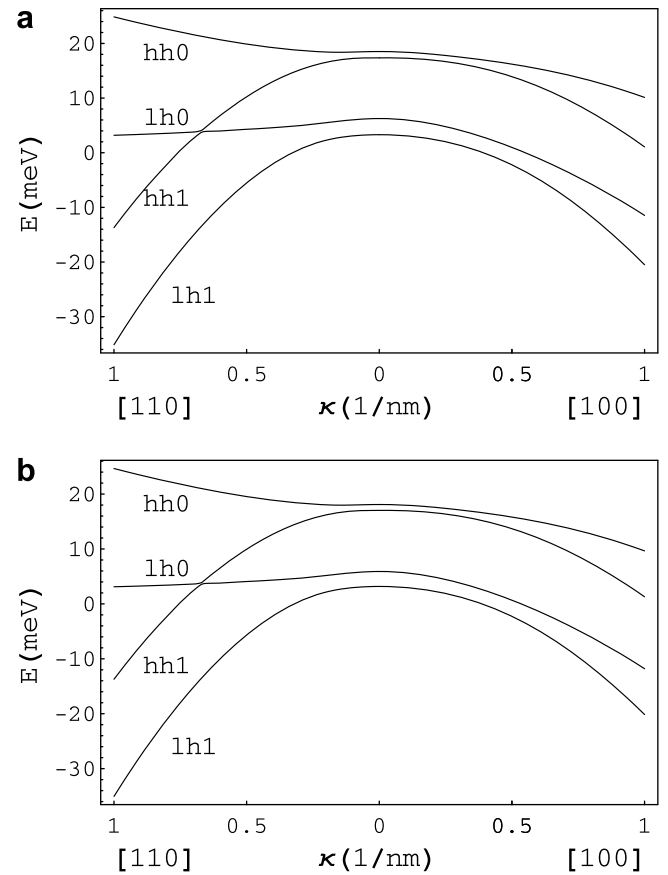

Fig. 4. Subband energy dispersion along two directions in the 2D Brillouin zone for a double δ-doped quantum well in Si. Doping concentration is $p_{2D} = 2.5 \times 10^{12}$ cm^{-2}, and the interwell distance is of 50 Å. Again, (a) corresponds to the set **I** of Luttinger parameters, and (b) is obtained with the set **II** of Luttinger parameters.

three values of the interwell distance $l = 30$ Å (a), $l = 50$ Å (b), and $l = 70$ Å (c). All these figures were generated with the use of the SLP **I**. The increase in the interwell distance causes little modifications regarding the position of the heavy and light holes ground states. However, the levels hh1 and lh1 substantially modify their values, becoming more localized states as long as the wells separate further. As can be seen, this provokes the shifting of the point in the direction [1 1 0] of the two-dimensional κ-space where the anticrossing between lh0 and hh1 states takes place. For larger the interwell distance, the closer to the zone center this point will be.

As it can be seen from the results obtained, no important differences are found when using distinct SLPs. This is obviously due to the similarity in the values of the Luttinger parameters in both cases. Appreciable changes would be noticed if both γ_2 and γ_3 were significantly different from one SLP to the other.

As we pointed out, for the values of the two-dimensional carrier concentration considered in the work, it is assumed that the split-off band is empty of charge. This would justify the use of the 4×4 Luttinger–Kohn description provided that the effect of the interaction with this third hole band could be neglected. But it is apparent from our numerical output that the approximation is failing in some way, giving the unphysical negative effective mass result very close to the Brillouin zone center for single δ-doped quantum wells. Indeed, the value of the spin-orbit splitting is not large for Si. Nevertheless, the coupling between split-off and heavy-hole bands may not be negligible. Then, even without population, the split-off band might be significantly affecting the subband structure of the single δ-well. It is worth mentioning that this situation has been already commented in Ref. [6], and seems not to be associated with any particular choice of the Luttinger parameters. However, the most interesting aspect of this problem is that it does not manifest at all in the case of double p-δ-doped Si quantum wells, in which case the combined effect of the deepening of the hh0 level position and the interaction between the subbands corresponding to different wells will be overcoming the possible influence of the split-off band.

4. Conclusions

We have used the 4 **k · p** Luttinger–Kohn model to study the hole subband structure in single and double p-type δ-doped quantum wells in Si. The use of approximate
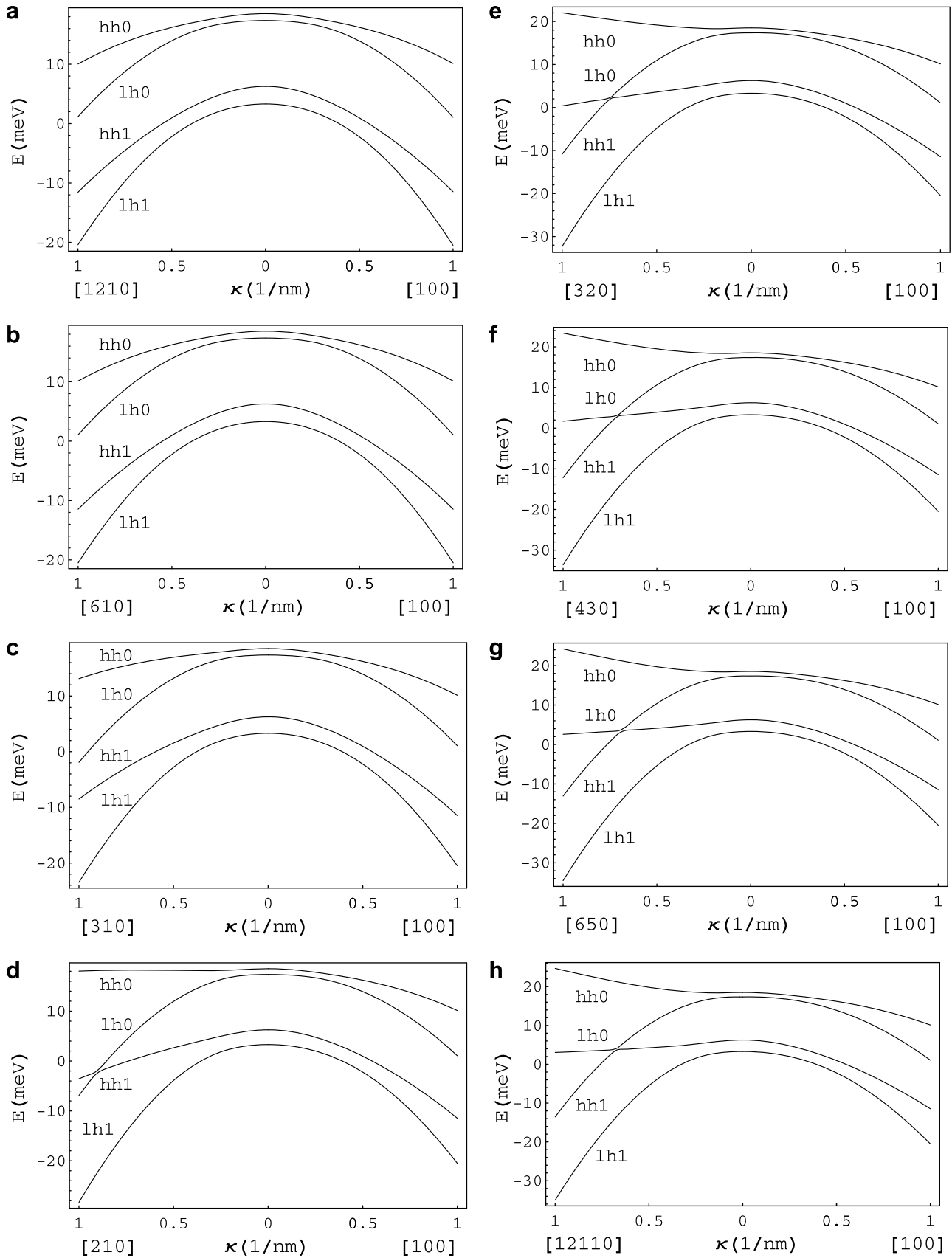
Fig. 5. Subband energy dispersion of double δ-doped quantum well in Si for eight different directions in the two-dimensional Brillouin zone, for angles between 0 and $\pi/4$. The doping concentration is $p_{2D} = 2.5 \times 10^{12}$ cm^{-2}, and the interwell distance is set to be 50 Å, for illustration. This figure corresponds to the set of Luttinger parameters labeled as **I**.
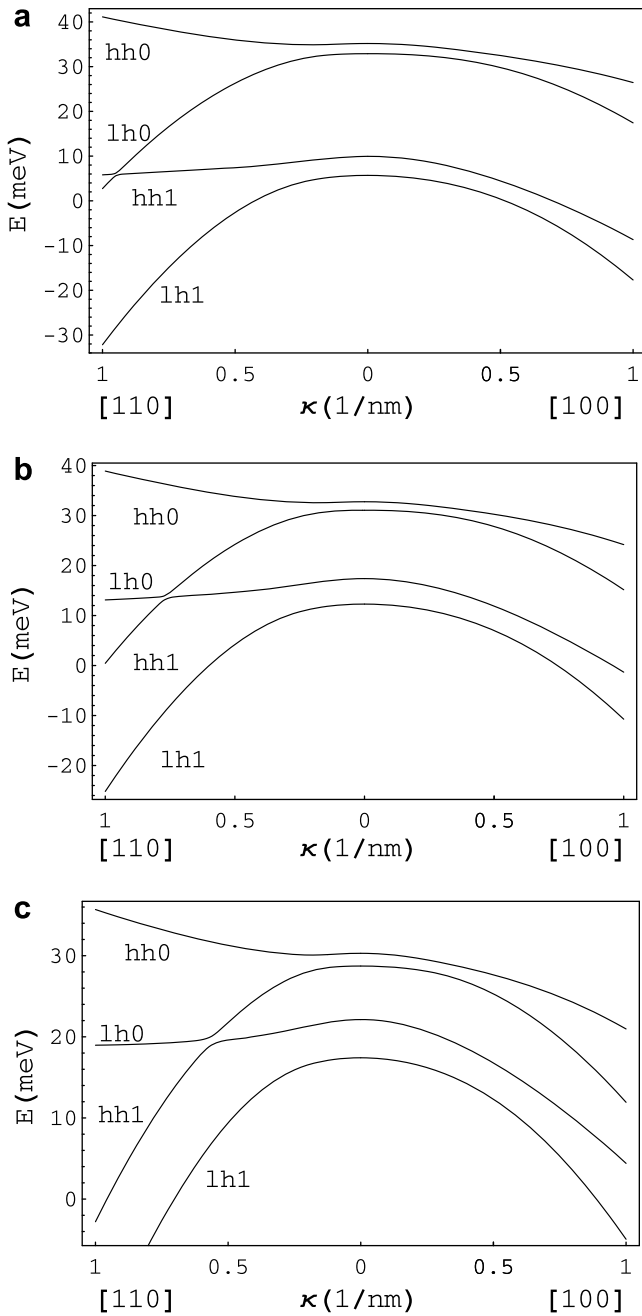
Fig. 6. Energy subband dispersion for Si double δ-doped quantum wells, obtained with the use of the set **I** of Luttinger parameters. $p_{2D} = 5 \times 10^{12}$ cm^{-2}. (a) $l = 30$ Å, (b) $l = 50$ Å, (c) $l = 70$ Å.

TF-type models for the description of hole energies in double Si p-type δ-doped quantum wells has been restricted to deal with zone-center states. Previous founds has allowed to establish that a Thomas–Fermi–Dirac approach leads to a better description of the hole level ladders for $\kappa = 0$ [21–23]. The results of the present work go beyond by extending such treatment to non-Γ states and show how the heavy, light hole subband spectra are affected by the interband interaction for states with two-dimensional wavevector close to the Γ point. This modification could be of importance for the optical properties associated with intersubband transitions. In this sense, the description of the hole energy structure is more complete. It is shown that the hole subband structure significantly depends upon the direction in the two-dimensional Brillouin zone, showing quite strong anti-crossings for directions approaching the K-point.

On the other hand, our results for the case of single δ-doped quantum wells suggest that the two-hole-bands approximation could be leading to a non-physical description of the heavy-hole ground state close to the Brillouin zone center and, consequently, a more complete **k · p** approach is required in this direction. In spite of this inconvenient, we believe that within the chosen approximation our procedure may provide a quite accurate and simple alternative of calculation, mainly in the case of double δ-doped systems.

Another conclusion arising from our calculations is that for the study of hole states on Si p-δ-doped systems, each of the two sets of Luttinger parameters considered can be used indistinctly.

Acknowledgement

References

[1] Wang KL, Karunasiri RPG, Park JS. Surf Sci 1992;267:74.
[2] Karunasiri G. Jpn J Appl Phys 1994;33:2401.
[3] Zhu JH, Gong DW, Zhang B, Lu F, Sheng C, Sun HH, et al. Phys Rev B 1995;52:8959.
[4] Siphai GM, Enderlein P, Scolfaro LMR, Leite JR. Phys Rev B 1996;53:9930.
[5] Gaggero-Sager LM, Pérez-Alvarez R. Appl Phys Lett 1997;70:212.
[6] Rosa AL, Scolfaro LMR, Enderlein R, Sipahi GM, Leite JR. Phys Rev B 1998;58(15):675.
[7] Gaggero-Sager LM, Mora-Ramos ME, Contreras-Solorio DA. Phys Rev B 1998;57:6286.
[8] Kaesen F, Fink C, Anil KG, Hansch W, Doll T, Grabolla T, et al. Thin Solid Films 1998;336:309.
[9] Gaggero-Sager LM, Mora-Ramos ME. Phys Status Solidi (b) 2000;220:163.
[10] Chien PW, Wu SL, Lee SC, Chang SJ. Mater Chem Phys 2002;77:426.
[11] Caro J, Vink ID, Smit GDJ, Rogge S, Klapwijk TM. Phys Rev B 2004;69:125324.
[12] Liu R, Wee ATS, Shen DH, Takenaka H. Surf Interface Anal 2004;36:172.
[13] Gaggero-Sager LM, Perez-Alvarez R. J Appl Phys 1995;78:4566.
[14] Martinez-Orozco JC, Gaggero-Sager LM, Vlaev SJ. Mater Sci Eng B 2001;84:155.
[15] Zheng X, Carns TK, Wang KL, Wu B. Appl Phys Lett 1993;62:504.
[16] Shieh HM, Hsu WC, Wu CL. Appl Phys Lett 1993;63:509.
[17] Wu CL, Hsu WC, Shieh HM, Liu WC. Appl Phys Lett 1994;64:3027.
[18] Sheih H-M, Wu C-L, Hsu W-C, Wu Y-H, Kao M-J. Jpn J Appl Phys 1994;33:1778.
[19] Gurtovoi VL, Valyaev VV, Shapoval SYu, Pustovit AN. Appl Phys Lett 1998;72:1202.
[20] Radamson HH, Sardela Jr MR, Nur O, et al. Appl Phys Lett 1994;64:1842.

[21] Rodriguez-Vargas I, Gaggero-Sager LM, Velasco VR. Surf Sci 2003;537:75.

[22] Rodriguez-Vargas I, Gaggero-Sager LM. Physica B 2007;389:227.

[23] Gaggero-Sager LM. Phys Status Solidi (b) 2002;231:243.

[24] Bobbert PA, Wieldraaijer H, van der Weide R, Kemerink M, Koenraad PM, Wolter JH. Phys Rev B 1997;56:3664; Combescot M, Nozieres P. J Phys C 1972;5:2369.

[25] Luttinger JM, Kohn W. Phys Rev 1955;97:869.

[26] Ma CS, Han CH, Liu SY. Opt Quantum Electr 1997;29:697.

[27] Rodriguez-Vargas I, Mora-Ramos ME. Superlattices Microstruct 2006;40:100.

[28] Harbeke G, Madelung O, Rössler U. In: Madelung O, editor. Numerical data and functional relationships in science and technology. Landolt-Börnstein, new series, group III, vol. 17. Berlin: Springer-Verlag; 1982.

[29] Yu P, Cardona M. Fundamentals of semiconductors. 2nd ed. Berlin: Springer-Verlag; 1999.